THE EUROPEAN SOCIETY OF MEDICINE
Medical Research Archives, Volume 13 Issue 6

RESEARCH ARTICLE

Mechanisms of Ultrasound-Enhanced Vascular Permeability

Afsana F. Islam, Tao Peng, David D. McPherson and Melvin E. Klegerman*

[1]Division of Cardiovascular Medicine, Department of Internal Medicine, University of Texas Health Science Center, Houston, TX 77030

*Melvin.E.Klegerman@uth.tmc.edu

OPEN ACCESS

PUBLISHED
30 June 2025

CITATION
Islam, A.F., Peng, T., et al., 2025. Mechanisms of Ultrasound-Enhanced Vascular Permeability. Medical Research Archives, [online] 13(6). https://doi.org/10.18103/mra.v13i6.6609

DOI
https://doi.org/10.18103/mra.v13i6.6609

ISSN
2375-1924

ABSTRACT

Both continuous- and pulsed-wave ultrasound have been shown to increase endothelial permeability to echogenic liposomes (ELIP) and stem cells associated with them *in vitro* and *in vivo*. We have been able to model this phenomenon *in vitro* with human umbilical vein endothelial cell (HUVEC) monolayers grown on transwell inserts. The ultrasound effect is not dependent on ELIP echogenicity, indicating that it is induced by radiation pressure, rather than by cavitation forces, and is blocked by N^G-nitro-L-arginine methyl ester, an inhibitor of endothelial nitric oxide synthase, establishing that it is mediated by nitric oxide signaling. Western blots of ultrasound-treated cultured HUVEC lysates and untreated controls indicated that nitric oxide activates the Akt pathway, implicating the intracellular transduction mechanism mediating shear stress effects on endothelial cells, but that other mechanoreceptor-triggered pathways may also be involved.

Keywords: ultrasound; vascular permeability; nitric oxide; liposomes

Introduction

When nitric oxide (NO) biochemical signaling was first discovered, it was shown to cause vascular dilation due to cyclic GMP-mediated relaxation of vascular smooth muscle cells[1,2]. Since then, NO has been shown to be a central mediator of normal vascular homeostasis, including several mechanisms of increased endothelial permeability[3]. One such mechanism is that mediating the atheroprotective effects of normal shear stress in arteries. It has been found that stimulation of mechanoreceptors on endothelial cell plasma membranes results in activation of Akt, eNOS and extracellular-regulated kinase 1/2 (ERK 1/2), leading to hyperpermeability[4,5], possibly mediated by phosphorylation of VE-cadherin and/or S-nitrosylation of β-catenin[6-8]. Intracellular NO generation is central to inhibition of atherogenesis, including antihypertensive, other cyclic guanosine monophosphate (cGMP)-mediated, antioxidative, anti-immune cell recruitment and anticytotoxic mechanisms [6,9-20].

Investigating diagnostic and therapeutic approaches to clinical atherosclerosis management, we have repeatedly shown that both NO-loaded echogenic liposomes (NO-ELIP) and ultrasound (US; continuous wave and pulsed Doppler) facilitate penetration of ELIP and even stem cells into vascular walls *in vivo* and transit across endothelial cell (EC) monolayers *in vitro* [21-24]. Simultaneous administration of intravascular ultrasound (IVUS) and an atheroma-targeted, pioglitazone-loaded ELIP formulation through an EKOS catheter immediately after stenting of atherosclerotic peripheral arteries in a miniswine model was significantly more efficacious in preventing reatherogenesis than administration of the same agent without ultrasound[25]. A study to confirm delivery of a fluorescently labeled analogous preparation to injured arterial endothelium in the same model showed that, in the absence of US, the agent adhered to the endothelial surface, while application of US forced it into the subsurface medial layer, indicating an increase in vascular wall permeability[23].

Ultrasound effects fall into two general categories, cavitation effects and radiation pressure. Cavitation describes the effects of US on gas bubbles; inertial cavitation involves bubble collapse that generates shock waves and stable cavitation creates bubble oscillations that result in microstreaming effects. While cavitation effects produce nanoscale pores in cell membranes that facilitate intracellular drug delivery, radiation pressure is more likely to mimic the permeability enhancement triggered by shear stress[26]. Hypothesizing that US-enhanced endothelial permeability is mediated by NO generation and signaling, in-part or completely involving shear stress-induced mechanisms, we conducted preliminary *in vitro* studies of cultured human umbilical cord endothelial cells (HUVEC) to answer these questions.

Materials and Methods

Preparation of Rhodamine-labeled Intercellular Adhesion Molecule-1 (ICAM-1)-targeted Echogenic Liposomes (Rho-AICAM1-ELIP) and Nitric Oxide-Loaded ELIP (NO-ELIP)

Intercellular adhesion molecule-1 (ICAM-1)-targeted ELIP were prepared as previously described [22] using ELIP containing 0.25 mole% Rhodamine B-phosphatidylethanolamine (PE). Thiolated antibody (anti-human ICAM-1) was conjugated to maleimide-derivatized ELIP (MPB-phosphatidylethanolamine) via a thioether linkage. For a control preparation, nonspecific murine immunoglobulin G (IgG) was conjugated to rhodamine-labeled ELIP (IgG-ELIP) instead of specific antibody. Nitric oxide-loaded ELIP (NO-ELIP) were also prepared as previously described[22]. The size distribution of IgG-ELIP and Ab-ELIP > 400 nm was determined with a Beckman Coulter Multisizer 3 instrument.

Assessment of Endothelial Permeability by Transwell Culture Methods

Human umbilical vein endothelial cells (HUVEC; PCS-100-013, American Type Culture Collection, Manassas, VA) were grown to confluence in 24-well transwell insert plates (8.0 μm pores, Corning, Inc., Kennebunk, ME). The cells were then treated with tumor necrosis factor-alpha (TNF-α; 20 ng/mL) to induce cell-surface expression of ICAM-1 and incubated overnight at 37°C in an atmosphere of 5% carbon dioxide (CO_2)/95% air. The insert plates and lower wells were washed with Dulbecco's phosphate-buffered saline (DPBS). The lower wells were refilled with 750 μL of endothelial cell medium (ECM), while the insert plates were treated with 120 μL (containing 120 μg lipid) of sterile Rho-AICAM1-ELIP or IgG-ELIP (negative control). For testing of cavitation effects, ELIP preparations were rendered non-echogenic by application of a 50% vacuum with a syringe for 1 minute (illustrated in Fig. 1). For inhibition studies,

10.0 μM N^G-nitro-L-arginine methyl ester (L-NAME), an inhibitor of endothelial nitric oxide synthase (eNOS)[27], or 1H-[1 ,2,4]Oxadiazolo[4,3-a]quinoxalin-1–one (ODQ; 0.1 and 1.0 μM), an inhibitor of soluble guanylyl cyclase (sGC) [28], was included in ECM at the time of ELIP incubation. For US treatment, 30 minutes after addition of ELIP, insert wells were treated with continuous-wave ultrasound (Sonitron 2000, RICH-MAR Co., Inola, OK) at 1 MHz, 2 W/cm^2, and 50% duty cycle for 1 minute. The insert plates were incubated for an additional 30 minutes at 37°C in the CO_2 incubator. The insert plates were then washed with DPBS, filled with 200 μL fresh ECM, and incubated for 24 hours. Aliquots (150 μl) of lower well media were transferred to opaque 96-well plates for measurement of fluorescence intensity (Ex 544 nm, Em 590 nm) with a SpectraMax M5 (Molecular Devices, San Jose, CA) microplate reader. To confirm confluency of the HUVEC monolayers, we added 2 μg of FITC-dextran 70 (Sigma-Aldrich, St. Louis, MO) to transwell inserts and measured the fluorescence intensity (Ex 485, Em 538) in the bottom wells at 0, 15, 30, 45, 60 and 120 minutes, using the microplate reader. Permeability values were calculated as described by Lal et al. [29]. To verify that intact liposomes passed through the monolayers, media in lower wells were examined by fluorescence microscopy (40X objective). Enumeration and size analysis of liposomes in insert and well media was performed with a Beckman Coulter Multisizer 4 instrument.

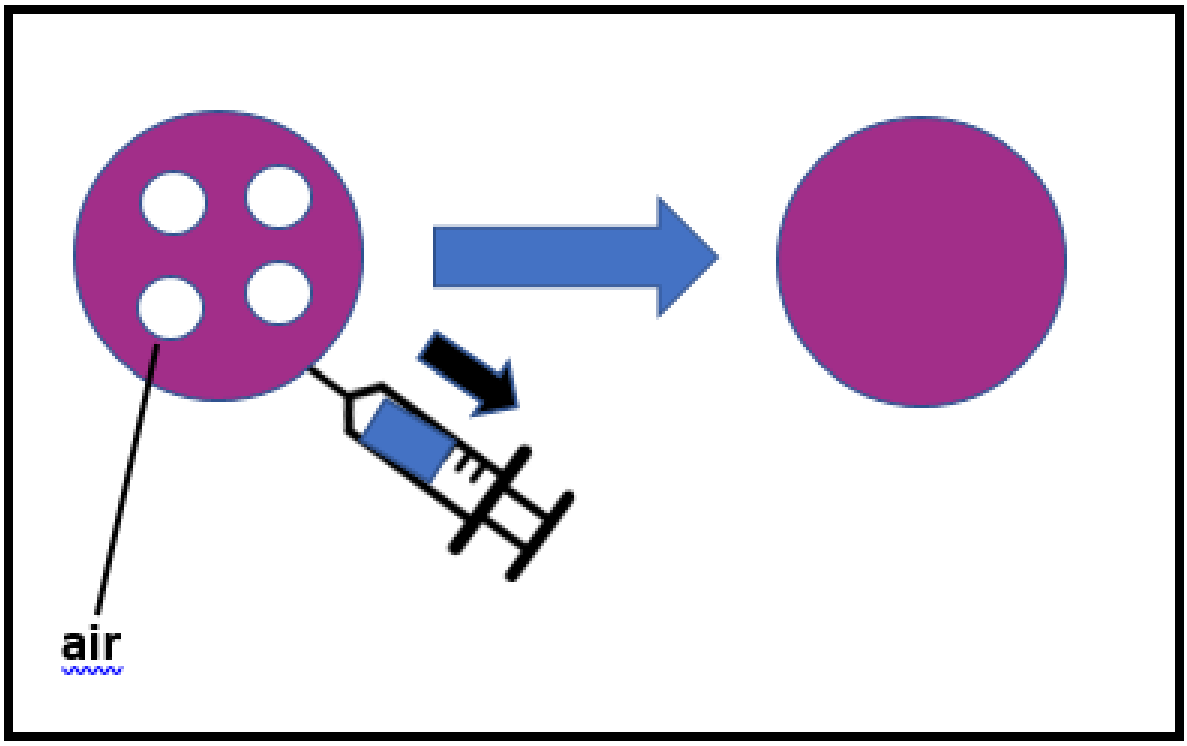

Figure 1. Illustration of air pockets in rhodamine-labeled ELIP being removed by 50% vacuum suction applied by a syringe, rendering the liposomes non-echogenic and unable to exhibit cavitation effects.

Quantitation of Intracellular Transduction Factors by Western Blot Analysis.

Confluent HUVEC in 6-well culture plates (Corning Inc., Corning, NY) were insonated as described for transwell cultures for various times ranging from 0 to 50 seconds. The cells were then incubated at 37°C with 5% CO_2 for 30 minutes and washed with DPBS twice; 100 μl of lysis buffer was added to each well, followed by gentle shaking for 10 minutes at room temperature. The lysates were transferred to Eppendorf tubes and placed on a tube rotator (Cole-Parmer, Vernon-Hills, IL) for 20 minutes at 4°C. Lysates were centrifuged (MIRKO 200R, Hettich, Tuttlingen, Germany) at 15,000 RPM for 10 minutes at 4°C. The supernatant was carefully pipetted into new Eppendorf tubes and the pellets were discarded. Lysates (normalized for protein content, determined by BioRad Dye Reagent) were denatured in water at 95°C for 5 minutes before loading onto 7.5% polyacrylamide gels (Bio-Rad Laboratories, Hercules, CA) for sodium dodecyl sulfate-polyacrylamide gel

electrophoresis (SDS-PAGE) before blotting onto polyvinylidene fluoride (PVDF) transfer membrane sheets (Thermo Fisher Scientific, Rockford, IL). Upon completion of the transfer, the PVDF membrane was blocked with blocking buffer (Odyssey-PBS, LI-COR, Lincoln, NE). Each section of the membrane was blotted with a different primary rabbit antibody overnight on a cell shaker (ProBlot Rocker 25, Labnet, Corning, Inc.) at 4°C: phospho-AKT (9271S, 1:500, Cell Signaling Technology) and AKT (9272S, 1:500, Cell Signaling Technology); phospho-ERK 1/2 (9101S, 1:500, Cell Signaling Technology) and ERK 1/2 (9102S, 1:500, Cell Signaling Technology); phospho-eNOS (PA5-104858, 1:200, Invitrogen) and eNOS (PA1-037, 1:500, Invitrogen); and beta-tubulin (ab6046, 1:2500, abcam). The integrity of the phospho-eNOS antibody was verified by fluorescent IHC staining of normal human lung sections (Fig. S1; see next section). For each primary antibody, a donkey-anti-rabbit secondary antibody that was coupled to infrared (IR) dyes (926-32213, 1:2500, LI-COR) was used. The blots were visualized with the LI-COR Odyssey Imaging System and then quantitated by densitometric analysis with NIH ImageJ software.

Immunohistochemical Validation of Phospho-eNOS Antibody.

Formalin-fixed, paraffin-embedded normal human lung sections were incubated with 1:500 diluted rabbit phospho-eNOS antibody in PBS at 4°C overnight, followed by 1:2000 goat anti-rabbit IgG conjugated to AlexaFluor 488 (Life technologies, Grand Island, NY, USA) at room temperature for 2 hours. Nuclei were stained with Antifade mounting medium with DAPI (VECTASHIELD Vibrance, Vector Laboratories Inc., Burlingame, CA, USA). Stained slides were examined and images collected with a fluorescent microscope (Nikon, eclipse Ti, Dusseldorf, Germany). Procurement of human tissues was approved by the UTHealth Committee for Protection of Human Subjects (HSC-MS-08-0354).

Statistics.

Replicate data were evaluated by normal variance analysis. Differences among populations were assessed by Student's t-test. A p-value ≤ 0.05 was considered significant.

Results

Ultrasound Application Facilitates Rho-AICAM1-ELIP (Ab-ELIP) Passage Through a HUVEC Monolayer.

Application of continuous wave ultrasound to HUVEC monolayers on transwell membranes significantly increased penetration of Ab-ELIP through the HUVEC monolayer compared to Ab-ELIP that did not undergo US treatment (Fig. 2; $p = 0.0002$). There was no significant difference in the US-enhanced penetration of non-echogenic Ab-ELIP relative to echogenic ELIP ($p = 0.57$; Fig.2), indicating that the effect is induced by radiation pressure, rather than cavitation processes. Four lots of IgG-ELIP measured with a Beckman Coulter Multisizer 3 instrument exhibited a mean spherical diameter of 780.5 ± 70.2 nm, while 5 lots of rhodamine-labeled anti-ICAM-1 conjugated ELIP had a mean spherical diameter of 781.8 ± 61.6 nm, which is also consistent with a radiation pressure-induced increase of paracellular transit, rather than intracellular passage. HUVEC monolayer confluence was confirmed by measurement of monolayer permeability to FITC-dextran 70. From the FITC-dextran flux across the transwell membrane between 30 and 120 minutes, we calculated a permeability of $4.1 \pm 0.3 \times 10^{-6}$ cm/sec (4 DOF), compared to $3.9 \pm 0.7 \times 10^{-6}$ cm/sec reported by Lal et al. [29] Fluorescence microscopy of media in the lower wells showed that liposomes as large as 3 μm in diameter passed through HUVEC monolayers after TNFα pretreatment (Fig. S2). In a separate experiment, Multisizer 4 analysis of media in both the inserts and the wells indicated that 67% of rhodamine-labeled ELIP with a median diameter of 481 μm passed into the wells with ultrasound treatment.

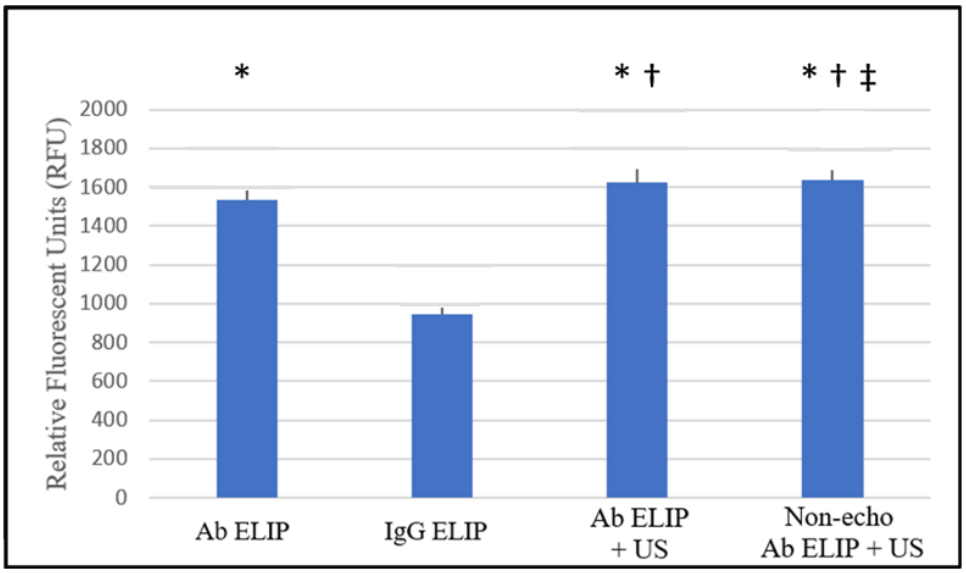

Figure 2. Evaluation of endothelial penetration and echogenicity of antibody-conjugated ELIP (Ab-ELIP) with ultrasound (US) treatment. * $p < 0.0001$ vs. IgG-ELIP; † $p < 0.005$ vs. Ab-ELIP; ‡ not significant vs. non-echo Ab-ELIP + US; 14 degrees of freedom (DOF; n = 8 per group) for each comparison.

Ultrasound-enhanced HUVEC Permeability is Mediated by Nitric Oxide (NO) Production.
Penetration of Ab-ELIP through US-treated HUVEC monolayers in the presence of 10 μM L-NAME showed that the endothelial NO synthase inhibitor L-NAME significantly suppressed the enhanced penetrative effect of ultrasound-treated Ab-ELIP ($p = 6.2 \times 10^{-5}$), similar to that of Ab-ELIP that did not receive ultrasound treatment ($p = 0.137$) (Fig. 3).

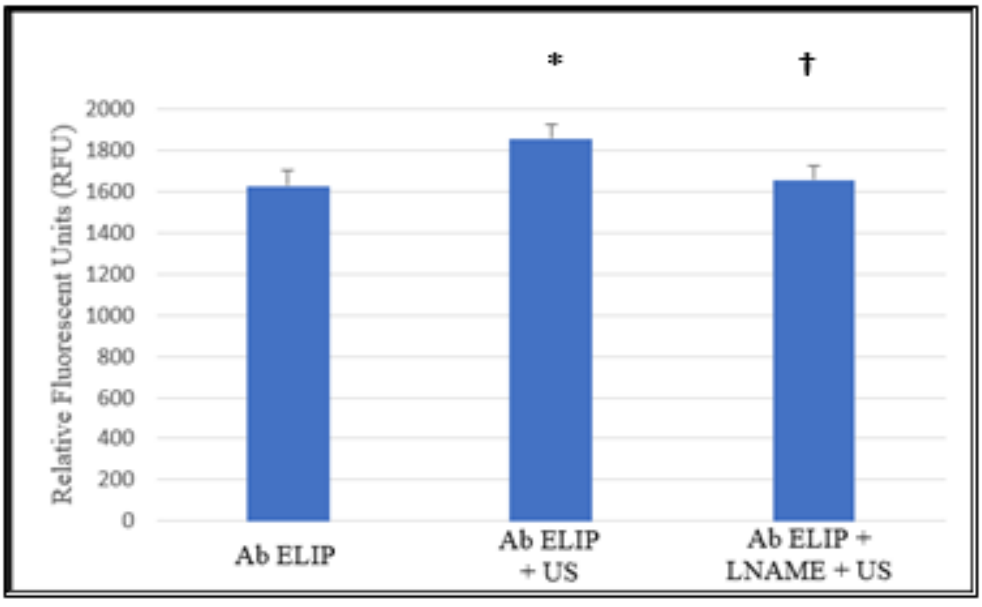

Figure 3. Dependence of ultrasound-enhanced endothelial penetration of Ab-ELIP on NO generation (n = 8-12). * $p < 0.0001$ vs. Ab-ELIP and Ab-ELIP + L-NAME + US; † NS vs. Ab-ELIP.

Ultrasound Enhancement of Vascular Permeability is Not Dependent on Cyclic GMP Activity.
Garthwaite showed that both 0.1 μM and 1.0 μM ODQ markedly inhibited cGMP production[28]. In preliminary experiments (data not shown), we found that 0.1 μM ODQ appeared to inhibit US enhancement of Ab-ELIP penetration more than 1.0 μM ODQ. However, repetition of the procedure showed that treatment of Ab-ELIP + US with 0.01-1.0 μM ODQ had no effect on the endothelial penetration of the fluorescent liposomes relative to Ab-ELIP + US (Fig. 4).

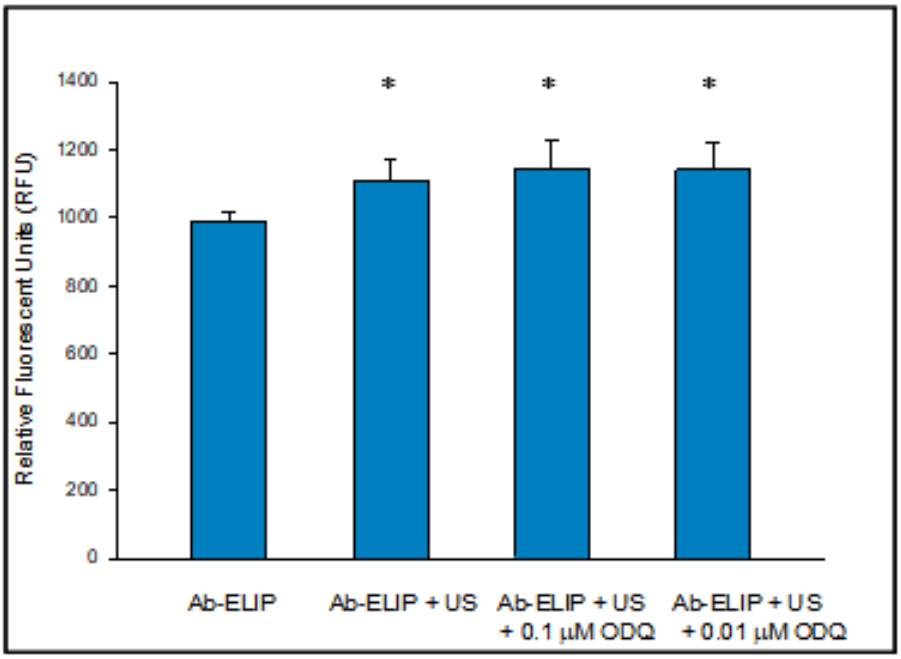

Figure 4. Evaluation of cGMP dependence of ultrasound enhancement of endothelial penetration (n = 8). * $p < 0.001$ vs. Ab-ELIP.

Ultrasound treatment greater than 50 seconds was toxic to HUVEC, as indicated by protein yields and microscopic examination. Ultrasound treatment of HUVEC caused phosphorylation of Akt and ERK 1/2 (normalized for total Akt and ERK 1/2, and β-tubulin levels), reaching maximum levels at 30 seconds of treatment (Fig. S3). Nine replicate 30-second US treatments of HUVEC cultures resulted in highly reproducible stimulation of Akt relative to 7 untreated controls (Fig. 5). Extracellular-regulated kinase 1/2 (ERK 1/2) stimulation under the same conditions was more marginal (Fig. 6), reflecting previous observations of equivocal effects on NO-dependent HUVEC monolayer permeability by ODQ, an inhibitor of the cyclic GMP pathway.

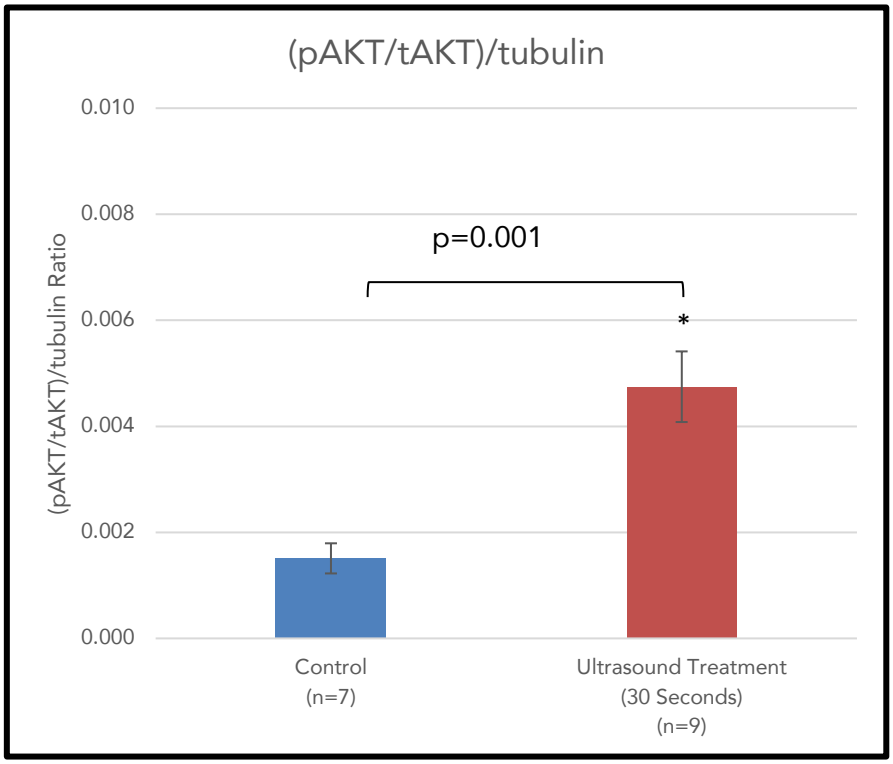

Figure 5. Quantitation of Western blots of phospho-Akt from replicate ultrasound treatment of HUVEC cultures for 30 seconds, demonstrating the reproducibility of the effect. Bars = mean ± SE.

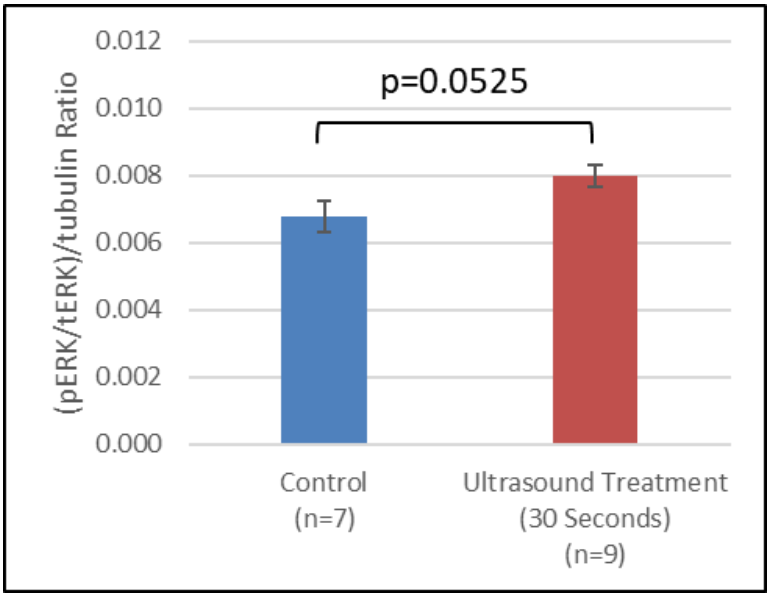

Figure 6 Quantitation of Western blots of phospho-ERK 1/2 from replicate ultrasound treatment of HUVEC cultures for 30 seconds. Bars = mean ± SE.

Ultrasound-Dependent Akt Activation Requires NO Production.

Treatment of HUVEC cultures with 10 μM L-NAME completely abolished the US-induced phosphorylation of Akt (Fig. 7A), indicating that NO production is necessary for Akt activation. N^G-nitro-L-arginine methyl ester (L-NAME) also inhibited the more marginal US-enhanced ERK 1/2 stimulation (Fig. 7B). We found that nitric oxide-loaded ELIP treatment of HUVEC cultures caused Akt phosphorylation (Fig. S4), confirming that NO production occurred before Akt activation. Western blotting of HUVEC lysates with antibodies specific for eNOS and phosphorylated eNOS indicated that eNOS phosphorylation did not occur in control or US-treated cells, but that US caused a significant increase of eNOS levels, suggesting constitutive stimulation of eNOS activity (Fig. 8).

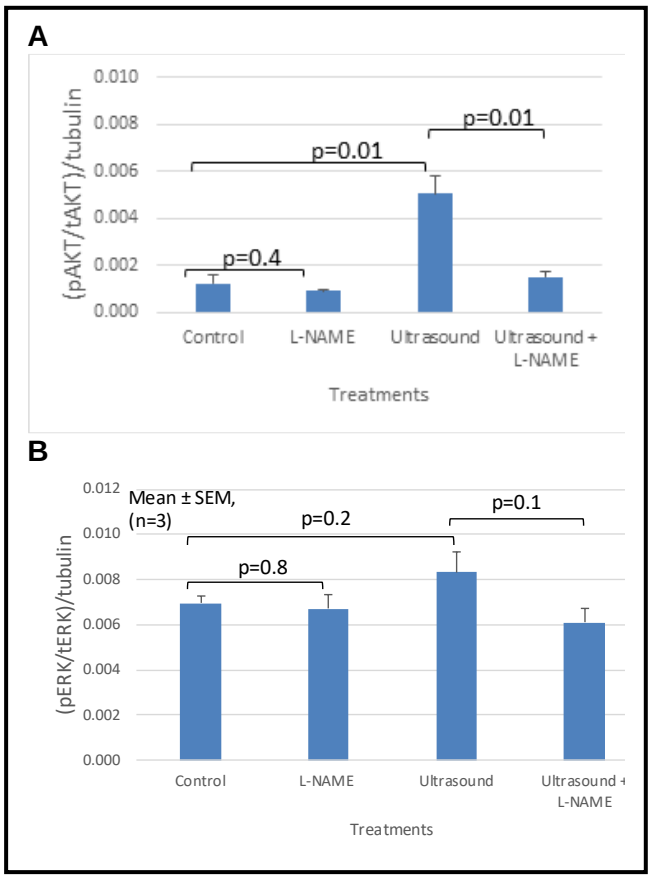

Figure 7. A. Effect of L-NAME on ultrasound-induced Akt phosphorylation, relative to total Akt and tubulin (n = 3). **B.** Effect of L-NAME on ultrasound-induced ERK 1/2 phosphorylation, relative to total ERK 1/2 and tubulin (n = 3).

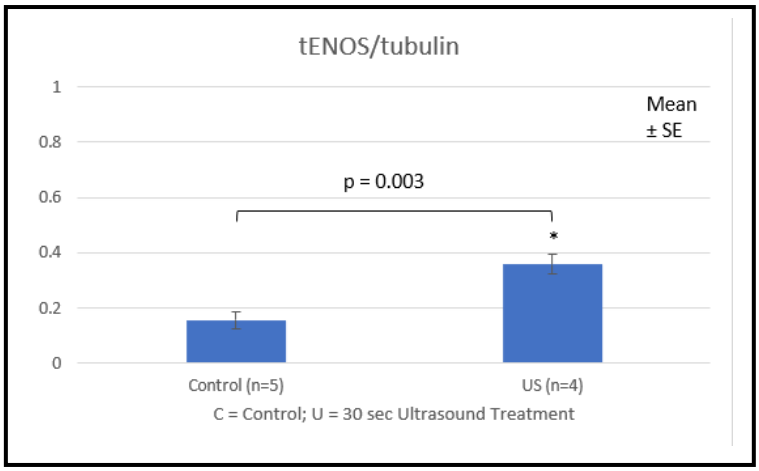

Figure 8. Ultrasound (US)-induced Increase in HUVEC eNOS Levels.

Discussion

Vascular permeability has become a subject of increasing interest. Once thought to be a derivative function of vasodilation, vascular permeability is now recognized as an integral aspect of inflammatory and atherogenic processes, mediated by distinct intracellular mechanisms. One of the best-studied mechanisms of enhanced endothelial permeability is shear stress produced by normal laminar flow. The pathway is initiated by the mechanical transduction receptor PIEZO 1, which causes a G_q/G_{11}-mediated Ca^{2+} influx, resulting in Akt phosphorylation mediated by Kruppel-like factors KLF2/KLF4 and Yes-associated protein/PDZ-binding motif (YAP/TAZ) [10,30-34]. Activated Akt phosphorylates endothelial nitric oxide synthase (eNOS), causing production of NO from L-arginine[5,9,12,15], which directly increases endothelial permeability, at least partly by causing phosphorylation of VE cadherin, and indirectly by activating ERK 1/2 through potentiation of soluble guanylyl cyclase (sGC) and the cyclic GMP pathway[5,33].

Although PIEZO 1 is recognized as the primary mechanotransduction receptor mediating wall shear stress (WSS) effects in vascular endothelium[35], several other molecules, such as platelet endothelial cell adhesion molecule-1 (PECAM-1) and various integrins (e.g., $\alpha_v\beta_3$) could perform a similar function[35,36]. In addition, the integrity of the cytoskeleton has been found to be necessary for WSS effects[37], suggesting that further investigation of the actomyosin network may elucidate other mechanotransduction receptors if PIEZO 1 is not found to mediate ultrasound effects. Our *in vitro* study of vascular permeability enhancement induced by continuous wave ultrasound appeared to involve transduction pathways mediating shear stress effects, but several important differences were noted. While we found that the effect, triggered by radiation forces, was mediated by NO production and resulted in Akt phosphorylation, the latter effect was dependent on NO production, indicating that, unlike shear stress effects, Akt did not stimulate eNOS activity. In this case, eNOS was constitutively induced by another mechanism. Others have reported that eNOS phosphorylation and NO production can be uncoupled. While adenosine triphosphate (ATP) and histamine caused both eNOS phosphorylation at Ser 1177 and NO production, vascular endothelial growth factor (VEGF), insulin, hydrogen peroxide and adenosine monophosphate kinase (AMPK) caused eNOS phosphorylation without NO production[38]. It is reasonable to expect that NO production can be elicited without eNOS phosphorylation. We also found that ERK 1/2 was marginally activated by phosphorylation, reflecting NO activation of soluble guanylyl cyclase (sGC), which catalyzes cyclic GMP (cGMP) production from GTP, resulting in downstream activation of mitogen-activated protein kinase 1/2 (MEK 1/2) and ERK 1/2[5], which increases endothelial permeability[5]. The muted ERK 1/2 response, compared to a more robust Akt stimulation, may be due to the relatively low abundance of sGC in endothelial cells[6].

Many recent studies have elucidated numerous cases of NO-induced activation of intra-cellular transduction factors by protein S-nitrosylation mechanisms, including those involved in regulation of endothelial permeability[5-7]. More than 3,000 peptides and proteins have been characterized and studied as S-nitrosylation targets[39]. These

mechanisms may mediate post-eNOS activation of Akt and permeability enhancement via S-nitrosylation of β-catenin variants[6,7], implicating the Wnt-canonical pathway as a modular network of alternative connections between cell-surface mechanoreceptors and intercellular junctions[40]. We did not observe phosphorylation of VE-cadherin (data not shown), suggesting that the permeability increase may be mediated by β-catenin activation or that a more definitive study of VE-cadherin activation over time is needed. It has been shown that nitric oxide can activate Src kinase, which in turn activates c-Src[41]. Src kinase phosphorylates eNOS in endothelial cells[42], yet we did not observe eNOS phosphorylation. Implications of this study for intracellular transduction pathways mediating ultrasound enhancement of endothelial permeability are summarized in Figure 9. It is most important at this point to 1) elucidate the afferent pathway by identifying the mechanotransducer impacted by ultrasound and the means by which eNOS is induced, 2) confirm that Src kinase is activated and determine why it does not initiate a feedback loop of eNOS activation, and 3) elucidate the efferent pathway by determining whether permeability enhancement is effected directly by NO through β-catenin S-nitrosylation. Once the major aspects of the pathway are known, ultrasound parameters can be optimized for maximum effectiveness.

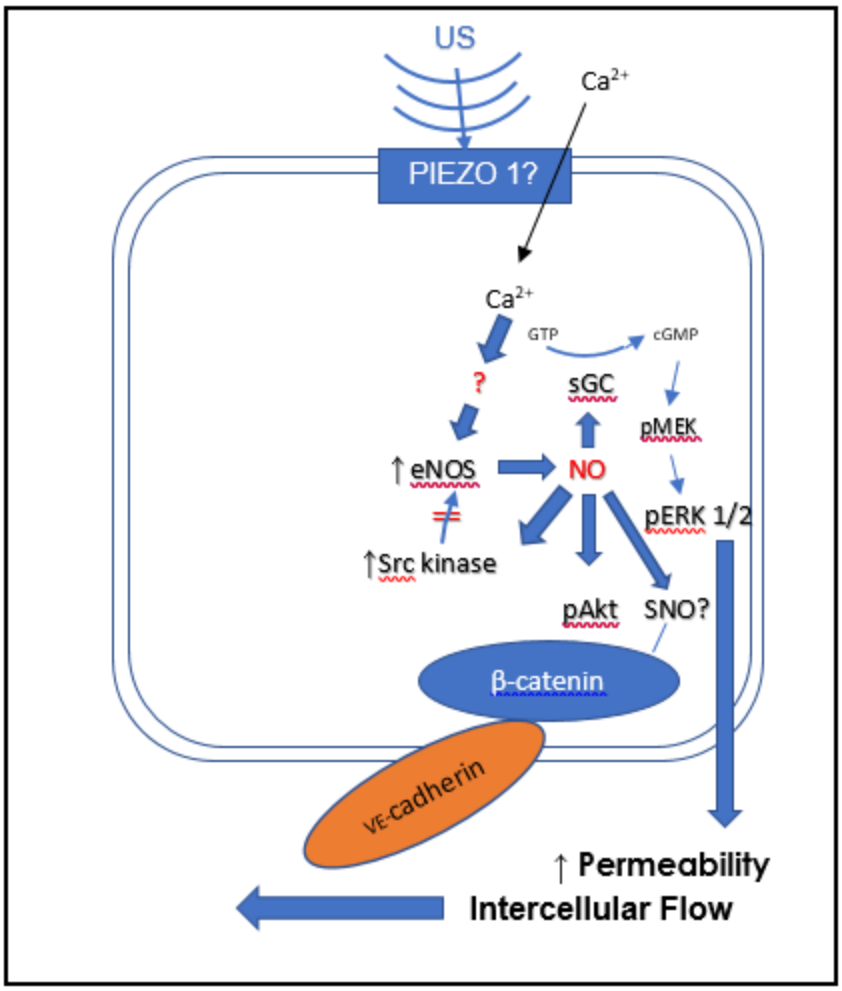

Figure 9. Schematic of prospective transduction pathways linking ultrasound (US) impaction of the endothelial cell surface and mechanisms of enhanced intercellular permeability. Abbreviations: cGMP, cyclic guanosine monophosphate; eNOS, endothelial nitric oxide synthase; GTP, guanosine triphosphate; NO, nitric oxide; pERK 1/2, phosphorylated extracellular signal-regulated kinase 1/2; pMEK, phosphorylated MAP2 kinase genes; sGC, soluble guanylyl cyclase; SNO, S-nitrosylate; US, ultrasound.

While the gap junctions between endothelial cells are normally only several nanometers wide, the phenomenon of whole cell passage through endothelial cell layers, known as extravasation, is well-established, both *in vivo* and *in vitro*. As reviewed by Salminen *et al.* [43], capture of leukocytes by integrins such as ICAM-1 precedes transendothelial migration paracellularly (in 70-

90% of cases) through channels controlled by VE-cadherin and β-catenin[8]. As noted, we have previously demonstrated enhanced passage of CD34+ monocytes through confluent HCAEC monolayers in the transwell system by complexation of the monocytes with bifunctionally targeted ELIP and NO-ELIP[24]. In that case, we confirmed the mononuclear cell morphology of cells migrating through the membrane by microscopy. In this study, we demonstrated that intact liposomes traversed the HUVEC monolayer. Tumor Necrosis Factor α exposure of endothelial cells triggers a process including ICAM-1 expression and binding that reconfigures adherens junctions to allow passage of cells and particles through gaps of several hundred nanometers to 2 microns[44,45].

The results of this study indicate that the acoustic radiation pressure produced in a controlled manner by a clinical ultrasound probe should be proportional to measures of vascular permeability and levels of intracellular transduction factors mediating the effect. Once the precise nature of the quantitative relation between the ultrasound input and various outcome parameters is known, reproducible approaches to ultrasound-enhanced delivery of therapeutics, including drugs, genes, oligonucleotides, bioactive peptides and gases, stem cells, and nanoparticulate formulations of these entities to the vascular wall can be designed. A detailed knowledge of the intracellular pathways mediating ultrasound-enhanced vascular permeability is important, since it is becoming increasingly evident that any kind of mechanical perturbation of cell membranes has a complex variety of output effects, including cell proliferation, migration, motility, changes in intercellular permeability, and cell transformations resulting in inflammation, fibrosis, neovascularization, vascular dysfunction, and various pathological processes.

These mechanical perturbations fall into four major types that can be classified as hydrostatic pressure, fluid shear stress (FSS), tensile force and extracellular matrix (ECM) stiffness[35]. Factors mediating the effects of FSS have been summarized here, but the other mechanical impacts can be communicated by PECAM-, actomyocin- and integrin-mediated mechanisms, linked to various transduction factors and result in diverse outcomes. Ultrasound impacts on endothelial cell membranes are different in quality from FFR and have features in common with other types of mechanical stimuli. Elucidation of pathways mediating ultrasound-enhanced vascular permeability will thus provide additional insights into the complex and interesting network of intracellular effectors linking mechanical impacts with their physiological and pathological outcomes.

Conclusions

An *in vitro* study of ultrasound-enhanced vascular permeability utilizing human umbilical vein endothelial cell (HUVEC) transwell cultures demonstrated that US permeability enhancement is due to radiation pressure and is mediated by nitric oxide (NO) signaling. Western blot analysis of HUVEC cultures subjected to continuous wave US established that Akt and, to a lesser extent, ERK 1/2 phosphorylation were involved in the effect. Unexpectedly, Akt phosphorylation was found to be a consequence, rather than a precursor of NO generation, indicating that critical steps in the transduction pathway may involve protein nitrosylations. While phosphorylation of VE-cadherin could not be demonstrated in this study, more studies will be required to determine whether VE-cadherin and/or β-catenin are involved in direct mediation of paracellular permeability. While certain aspects of US-enhanced endothelial permeability are similar to those mediating shear stress-induced permeability effects, other aspects differ, underscoring the complexity of intracellular mechanotransduction pathways.

Supplementary Materials:

Figure S1: Normal human lung stained with phospho-eNOS antibody as described in Methods, **Figure S2:** Passage of rhodamine-labeled ELIP (Rho-ELIP) through HUVEC monolayers on transwell membranes after TNFα pretreatment, **Figure S3:** Composite quantitation of Western blots of HUVEC lysates after treatment with continuous wave ultrasound (US) for various durations, stained for phospho-Akt, relative to total Akt and β-tubulin, and phospho-ERK 1/2, relative to total ERK 1/2 and β-tubulin, **Figure S4:** Phospho-Akt response to treatment of HUVEC cell cultures with 0.5 mg NO-ELIP lipid/ml.

Author Contributions:

Conceptualization, A.F.I., T.P. and M.E.K.; methodology, A.F.I. and T.P.; investigation, A.F.I. and T.P.; writing—original draft preparation, A.F.I. and M.E.K.;

writing—review and editing, A.F.I., T.P., D.D.M. and M.E.K.; supervision, D.D.M. and M.E.K.; project administration, D.D.M. and M.E.K.; funding acquisition, D.D.M. All authors have read and agreed to the published version of the manuscript.

Funding:

This research received no external funding.

Institutional Review Board Statement:

The study was conducted in accordance with the Declaration of Helsinki, and approved by the Institutional Review Board of the University of Texas Health Science Center at Houston (protocol number HSC-MS-08-0354).

Acknowledgments:

We wish to thank Drs. Harry Karmouty-Quintana and Dewei Ren for providing fixed normal human lung sections that were used to validate the anti-phospho-eNOS antibody. This article contains data and information included in abstracts and posters entitled "Assessment of ultrasound-facilitated endothelial permeability using transwell culture methodology" and "In vitro implication of mechanisms mediating ultrasound-enhanced vascular permeability," which were presented at American Heart Association Vascular Discovery meetings in Seattle, WA (May 2022), and Boston, MA (May 2023), respectively[46,47].

Conflicts of Interest:

Drs. McPherson and Klegerman have research-related interests in Zymo Pharmaceuticals, LLC, including stock ownership and board service. This company had no role in the design of the study; in the collection, analyses, or interpretation of data; in the writing of the manuscript; or in the decision to publish the results.

References:

1. Ignarro LJ. Endothelium-derived nitric oxide: pharmacology and relationship to the actions of organic nitrate esters. *Pharm Res*. Aug 1989; 6(8):651-9. doi:10.1023/a:1015926119947

2. Moncada S, Palmer RM, Higgs EA. The discovery of nitric oxide as the endogenous nitrovasodilator. *Hypertension*. Oct 1988;12(4):365-72. doi:10.1161/01.hyp.12.4.365

3. Yue W, Li Y, Ou D, Yang Q. The GLP-1 receptor agonist liraglutide protects against oxidized LDL-induced endothelial inflammation and dysfunction via KLF2. *IUBMB Life*. Sep 2019;71(9):1347-1354. doi:10.1002/iub.2046

4. Dimmeler S, Assmus B, Hermann C, Haendeler J, Zeiher AM. Fluid shear stress stimulates phosphorylation of Akt in human endothelial cells: involvement in suppression of apoptosis. *Circ Res*. Aug 10 1998;83(3):334-41. doi:10.1161/01.res.83.3.334

5. Duran WN, Breslin JW, Sanchez FA. The NO cascade, eNOS location, and microvascular permeability. *Cardiovasc Res*. Jul 15 2010; 87(2):254-61. doi:10.1093/cvr/cvq139

6. Duran WN, Beuve AV, Sanchez FA. Nitric oxide, S-nitrosation, and endothelial permeability. *IUBMB Life*. Oct 2013;65(10):819-26. doi:10.1002/iub.1204

7. Thibeault S, Rautureau Y, Oubaha M, et al. S-nitrosylation of beta-catenin by eNOS-derived NO promotes VEGF-induced endothelial cell permeability. *Mol Cell*. Aug 13 2010;39(3):468-76. doi:10.1016/j.molcel.2010.07.013

8. Gavard J. Endothelial permeability and VE-cadherin: a wacky comradeship. *Cell Adh Migr*. 2014;8(2):158-64. doi:10.4161/cam.29026

9. De Caterina R, Libby P, Peng HB, et al. Nitric oxide decreases cytokine-induced endothelial activation. Nitric oxide selectively reduces endothelial expression of adhesion molecules and proinflammatory cytokines. *J Clin Invest*. Jul 1995;96(1):60-8. doi:10.1172/JCI118074

10. Dimmeler S, Fleming I, Fisslthaler B, Hermann C, Busse R, Zeiher AM. Activation of nitric oxide synthase in endothelial cells by Akt-dependent phosphorylation. *Nature*. Jun 10 1999;399(6736): 601-5. doi:10.1038/21224

11. Fulton D, Gratton JP, McCabe TJ, et al. Regulation of endothelium-derived nitric oxide production by the protein kinase Akt. *Nature*. Jun 10 1999;399(6736):597-601. doi:10.1038/21218

12. Gao F, Lucke-Wold BP, Li X, et al. Reduction of Endothelial Nitric Oxide Increases the Adhesiveness of Constitutive Endothelial Membrane ICAM-1 through Src-Mediated Phosphorylation. *Front Physiol*. 2017;8:1124. doi:10.3389/fphys.2017.01124

13. He H, Oo TL, Huang W, He LF, Gu M. Nitric oxide acts as an antioxidant and inhibits programmed cell death induced by aluminum in the root tips of peanut (Arachis hypogaea L.). *Sci Rep*. Jul 2 2019; 9(1):9516. doi:10.1038/s41598-019-46036-8

14. He P, Zeng M, Curry FE. cGMP modulates basal and activated microvessel permeability independently of [Ca2+]i. *Am J Physiol*. Jun 1998;274(6):H1865-74. doi:10.1152/ajpheart.1998.274.6.H1865

15. Hummel SG, Fischer AJ, Martin SM, Schafer FQ, Buettner GR. Nitric oxide as a cellular antioxidant: a little goes a long way. *Free Radic Biol Med*. Feb 1 2006;40(3):501-6. doi:10.1016/j.freeradbiomed.2005.08.047

16. Palmer RM, Ferrige AG, Moncada S. Nitric oxide release accounts for the biological activity of endothelium-derived relaxing factor. *Nature*. Jun 11-17 1987;327(6122):524-6. doi:10.1038/327524a0

17. Varma S, Breslin JW, Lal BK, Pappas PJ, Hobson RW, 2nd, Duran WN. p42/44MAPK regulates baseline permeability and cGMP-induced hyperpermeability in endothelial cells. *Microvasc Res*. Mar 2002;63(2): 172-8. doi:10.1006/mvre.2001.2381

18. Wink DA, Hanbauer I, Krishna MC, DeGraff W, Gamson J, Mitchell JB. Nitric oxide protects against cellular damage and cytotoxicity from reactive oxygen species. *Proc Natl Acad Sci U S A*. Nov 1 1993;90(21):9813-7. doi:10.1073/pnas.90.21.9813

19. Wink DA, Hines HB, Cheng RY, et al. Nitric oxide and redox mechanisms in the immune response. *J Leukoc Biol*. Jun 2011;89(6):873-91. doi:10.1189/jlb.1010550

20. Wink DA, Miranda KM, Espey MG, et al. Mechanisms of the antioxidant effects of nitric oxide. *Antioxid Redox Signal*. Apr 2001;3(2):203-13. doi:10.1089/152308601300185179

21. Herbst SM, Klegerman ME, Kim H, et al. Delivery of stem cells to porcine arterial wall with echogenic liposomes conjugated to antibodies against CD34 and intercellular adhesion molecule-1. *Mol Pharm*. Feb 1 2010;7(1):3-11. doi:10.1021/mp900116r

22. Kim H, Kee PH, Rim Y, et al. Nitric oxide improves molecular imaging of inflammatory atheroma using targeted echogenic immunoliposomes. *Atherosclerosis*. Dec 2013;231(2):252-60. doi:10.1016/j.atherosclerosis.2013.09.026

23. Klegerman ME, Moody MR, Huang SL, et al. Demonstration of ultrasound-mediated therapeutic delivery of fibrin-targeted pioglitazone-loaded echogenic liposomes into the arterial bed for attenuation of peri-stent restenosis. *J Drug Target*. Jan 2023;31(1):109-118. doi:10.1080/1061186X.2022.2110251

24. Klegerman ME, Wassler M, Huang SL, et al. Liposomal modular complexes for simultaneous targeted delivery of bioactive gases and therapeutics. *J Control Release*. Mar 19 2010;142(3):326-31. doi:10.1016/j.jconrel.2009.10.037

25. Kee PH, Moody MR, Huang SL, et al. Stabilizing Peri-Stent Restenosis Using a Novel Therapeutic Carrier. *JACC Basic Transl Sci*. Jan 2020;5(1):1-11. doi:10.1016/j.jacbts.2019.09.005

26. Husseini GA, Pitt WG, Martins AM. Ultrasonically triggered drug delivery: breaking the barrier. *Colloids /Surfaces B, Biointerfaces*. Nov 1 2014; 123:364-86. doi:10.1016/j.colsurfb.2014.07.051

27. Rees DD, Palmer RM, Schulz R, Hodson HF, Moncada S. Characterization of three inhibitors of endothelial nitric oxide synthase in vitro and in vivo. *Br J Pharmacol*. Nov 1990;101(3):746-52. doi:10.1111/j.1476-5381.1990.tb14151.x

28. Garthwaite J, Southam E, Boulton CL, Nielsen EB, Schmidt K, Mayer B. Potent and selective inhibition of nitric oxide-sensitive guanylyl cyclase by 1H-[1,2,4]oxadiazolo[4,3-a]quinoxalin-1-one. *Mol Pharmacol*. Aug 1995;48(2):184-8.

29. Lal BK, Varma S, Pappas PJ, Hobson RW, 2nd, Duran WN. VEGF increases permeability of the endothelial cell monolayer by activation of PKB/akt, endothelial nitric-oxide synthase, and MAP kinase pathways. *Microvasc Res*. Nov 2001;62(3):252-62. doi:10.1006/mvre.2001.2338

30. Dabravolski SA, Sukhorukov VN, Kalmykov VA, Grechko AV, Shakhpazyan NK, Orekhov AN. The Role of KLF2 in the Regulation of Atherosclerosis Development and Potential Use of KLF2-Targeted Therapy. *Biomedicines*. Jan 24 2022;10(2) doi:10.3390/biomedicines10020254

31. Fleming I. Molecular mechanisms underlying the activation of eNOS. *Pflugers Arch*. May 2010; 459(6):793-806. doi:10.1007/s00424-009-0767-7

32. Li J, Hou B, Tumova S, et al. Piezo1 integration of vascular architecture with physiological force. *Nature*. Nov 13 2014;515(7526):279-282. doi:10.1038/nature13701

33. Tamargo IA, Baek KI, Kim Y, Park C, Jo H. Flow-induced reprogramming of endothelial cells in atherosclerosis. *Nat Rev Cardiol*. Nov 2023; 20(11):738-753. doi:10.1038/s41569-023-00883-1

34. Wang S, Chennupati R, Kaur H, Iring A, Wettschureck N, Offermanns S. Endothelial cation channel PIEZO1 controls blood pressure by mediating flow-induced ATP release. *J Clin Invest*. Dec 1 2016;126(12):4527-4536. doi:10.1172/JCI87343

35. Di X, Gao X, Peng L, et al. Cellular mechanotransduction in health and diseases: from molecular mechanism to therapeutic targets. *Signal Transduct Target Ther*. Jul 31 2023;8(1):282. doi:10.1038/s41392-023-01501-9

36. Roux E, Bougaran P, Dufourcq P, Couffinhal T. Fluid Shear Stress Sensing by the Endothelial Layer. *Front Physiol*. 2020;11:861. doi:10.3389/fphys.2020.00861

37. Sun D, Huang A, Sharma S, Koller A, Kaley G. Endothelial microtubule disruption blocks flow-dependent dilation of arterioles. *Am J Physiol Heart Circ Physiol*. May 2001;280(5):H2087-93. doi:10.1152/ajpheart.2001.280.5.H2087

38. Eroglu E, Saravi SSS, Sorrentino A, Steinhorn B, Michel T. Discordance between eNOS phosphorylation and activation revealed by multispectral imaging and chemogenetic methods. *Proc Natl Acad Sci U S A*. Oct 1 2019;116(40):20210-20217. doi:10.1073/pnas.1910942116

39. Devarie-Baez NO, Zhang D, Li S, Whorton AR, Xian M. Direct methods for detection of protein S-nitrosylation. *Methods*. Aug 1 2013;62(2):171-6. doi:10.1016/j.ymeth.2013.04.018

40. Ferreira Tojais N, Peghaire C, Franzl N, et al. Frizzled7 controls vascular permeability through the Wnt-canonical pathway and cross-talk with endothelial cell junction complexes. *Cardiovasc Res*. Jul 15 2014;103(2):291-303. doi:10.1093/cvr/cvu133

41. da Costa PE, Batista WL, Moraes MS, Stern A, Monteiro HP. Src kinase activation by nitric oxide promotes resistance to anoikis in tumour cell lines. *Free Radic Res*. May 2018;52(5):592-604. doi:10.1080/10715762.2018.1455095

42. Haynes MP, Li L, Sinha D, et al. Src kinase mediates phosphatidylinositol 3-kinase/Akt-dependent rapid endothelial nitric-oxide synthase activation by estrogen. *J Biol Chem*. Jan 24 2003;278(4): 2118-23. doi:10.1074/jbc.M210828200

43. Salminen AT, Allahyari Z, Gholizadeh S, et al. In vitro Studies of Transendothelial Migration for Biological and Drug Discovery. *Front Med Technol*. 2020;2:600616. doi:10.3389/fmedt.2020.600616

44. Winger RC, Koblinski JE, Kanda T, Ransohoff RM, Muller WA. Rapid remodeling of tight junctions during paracellular diapedesis in a human model of the blood-brain barrier. *J Immunol*. Sep 1 2014; 193(5):2427-37. doi:10.4049/jimmunol.1400700

45. Yang L, Froio RM, Sciuto TE, Dvorak AM, Alon R, Luscinskas FW. ICAM-1 regulates neutrophil adhesion and transcellular migration of TNF-alpha-activated vascular endothelium under flow. *Blood*. Jul 15 2005;106(2):584-92. doi:10.1182/blood-2004-12-4942

46. Islam AF, Peng T, McPherson DD, Klegerman ME. In vitro implication of mechanisms mediating ultrasound-enhanced vascular permeability. *Arterioscl Thromb Vasc Biol*. 2023;43(1):A652.

47. Islam AF, Peng T, Shelat HS, et al. Assessment of ultrasound-facilitated endothelial permeability using transwell culture methodology. *Arterioscl Thromb Vasc Biol*. 2022;42(1):375.

